Journal of Engineering Mathematics **43:** 89–99, 2002.

Waves and singularities in nonlinear capillary free-surface flows

S. TOOLEY and J.-M. VANDEN-BROECK
School of Mathematics, University of East Anglia, Norwich NR4 7TJ, U.K.

Received 4 July 2001; accepted in revised form 4 March 2002

Abstract. The problem is a free-surface flow of a fluid, emerging from a semi-infinite container. The fluid is assumed to be inviscid, incompressible and the flow to be two dimensional and irrotational. When surface tension is neglected the free surface leaves the wall of the container tangentially. We show that when surface tension is taken into account, there is, in general, a train of waves on the free surface and a discontinuity in slope where the free surface separates from the wall of the container. These new solutions include, as particular cases, previously obtained solutions for which the free surface is waveless in the far field. Although the calculations are presented for a special flow configuration, the results are general and apply to other potential free surface flows where a free-surface intersects a rigid wall.

Key words: free surface, integral equations, surface tension, waves

1. Introduction

Many applications in fluid mechanics involve intersections of free surfaces and rigid surfaces. A classical example is the flow generated by a ship or an obstacle moving at the surface of water. Here the intersection is the water line where the surface of the water intersects the hull of the ship. In this paper we restrict our attention to two-dimensional potential flows. We present new results on the nature of the singularities which can occur at the intersection of free and rigid surfaces when surface tension is taken into account. As we shall see, the strength of these singularities is related to the possible presence of capillary waves on the free surfaces.

We present our results by using the specific flow configuration in Figure 1. This is a flow bounded by two walls AB and BC and a bottom EF. We have a free surface CD, which separates from the vertical wall BC at point C, ($x = y = 0$), but is unbounded as $x \to \infty$. However, the results are general and apply to other flows in which free surfaces intersect rigid surfaces. The flow of Figure 1 has several interpretations. Firstly, it represents a free-surface flow emerging from a container. Secondly, if we reflect the flow into the boundary AB, we obtain an open-wake model for the cavitating flow past a vertical plate in a channel. Thirdly, we can reverse the direction of the flow in Figure 1, and obtain a model for a 'bow flow' (*i.e.* the flow near the front of an object moving at a constant velocity at the surface of a fluid when viewed in a frame of reference moving with the object). Finally if B coincides with C, the model represents a flow past a flat plate.

When surface tension is neglected, an exact 'free streamline' solution for the flow of Figure 1 can be obtained by using conformal mappings. This solution shows that the free surface has a continuous slope and an infinite curvature at the separation point C (see Figure 1). The singularity in curvature is not troublesome when surface tension is neglected because the curvature of the free surface does not appear in the boundary conditions. However, when surface tension is taken into account, the curvature of the free surface appears explicitly in the

dynamic boundary condition. Therefore we can expect the limit as $T \to 0$ to be a singular limit. This is confirmed by the analytical and numerical results of Ackerberg [1], Cumberbatch and Norbury [2], Vanden-Broeck [3] and Ackerberg and Liu [4].

Ackerberg [1] constructed a local asymptotic solution in the neighbourhood of the separation point C for small values of the surface tension. His profile of the free surface has a continuous slope at the separation point C and a train of small linear capillary waves on the free surface. Ackerberg's [1] solution is general in the sense that it applies locally to any free surface potential flow where a free-surface intersects a rigid surface. We note that capillary waves do not satisfy the radiation condition when the flow is to the right as in Figure 1. However, if the flow is to the left (*i.e.* if the direction of the flow in Figure 1 is reversed), then capillary waves are physically acceptable. In other words, there should be no waves on the free surface, if we interpret the flow of Figure 1 as a cavitation flow or as the flow from a container. On the other hand, waves are permitted if we interpret Figure 1 as a bow flow. We note that the bow-flow interpretation of Figure 1 is less realistic than the cavitation flow interpretation for the particular geometry of the walls AB and BC.

Cumberbatch and Norbury [2] concentrated on the case where no waves are allowed on the free surface and tried to construct an appropriate local asymptotic solution for small values of the surface tension. In their analysis they assume that the flow leaves the wall tangentially but no suitable inner solution near the separation point could be found.

Vanden-Broeck [3] used numerical procedures to construct fully nonlinear solutions without waves on the free surface. He found that the free surface does not leave the wall tangentially when surface tension is taken into account. The surface tension does not remove the infinite curvature of the free-streamline solution. In fact, it makes the problem more singular by introducing a discontinuity in slope and an infinite velocity at the point C. Vanden-Broeck [5], [3] showed that a flow in a corner is the appropriate inner solution to complete the calculations of Cumberbatch and Norbury [2]. He derived a complete asymptotic solution which agrees with his numerical results as $T \to 0$.

More recently, Andersson and Vanden-Broeck [6] obtained analytical and numerical solutions for the free-surface flow past a flat plate in water of infinite depth (*i.e.* the flow in Figure 1 when B coincides with C and $H = \infty$). They found that there is a one-parameter family of solutions with a train of capillary waves on the free surface and a discontinuty in slope at the separation point. By using conservation of momentum and the solution of Crapper [7], they derived an exact relation between the steepness of the waves and the angle between the free surface and the plate at C.

In this paper we combine the ideas described in the three previous paragraphs to construct a general family of solutions for the flow of Figure 1 in which we allow capillary waves on the free surface and a discontinuity in slope at the point C. To satisfy the radiation condition, the direction of the flow in Figure 1 should be reversed when there are waves on the free surface. If there are no waves, then the direction of the flow can be in either direction. We solve the problem numerically by a boundary-integral equation method. We show that there is a two-parameter family of solutions without waves but with a discontinuity in slope at C. This family reduces to the one-parameter family of solutions calculated by Vanden-Broeck [3] when $H = \infty$. Our main result is that there is a four-parameter family of solutions when both waves and a discontinuity in slope are allowed. This family includes as particular cases the two-parameter family of waveless solutions. The numerical method used is based on an integro-differential equation reformulation. Such an approach has been used by many previous

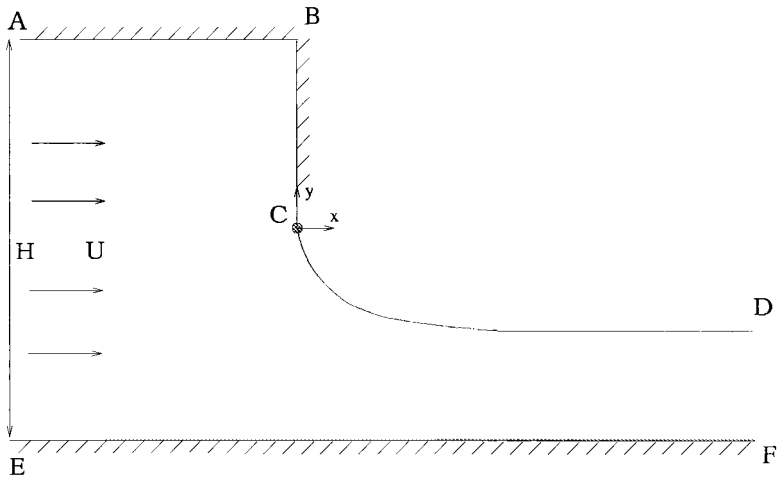

Figure 1. Sketch of the flow and the positioning of the coordinates.

investigators such as Forbes and Schwartz [8], Baker, Meiron and Orszag [9], Meiron and Saffman [10] and King and Bloor [11].

The presence of an infinite velocity at the separation point C is clearly not physically acceptable. It is therefore important to find ways to avoid these unbounded velocities. One possiblity is to replace the infinitely thin object ABC by an object with finite thickness and continuous slope. There is then an extra degree of freedom, namely the position of the separation point. Vanden-Broeck [12] showed that it is possible to use this degree of freedom to eliminate the discontinuity in slope (and the infinite velocity) at C. The results in this paper provide another possibility: we can try to select among the four-parameter family of solutions particular solutions for which the angle between the rigid wall and the free surface at C is zero. These solutions can be viewed as a nonlinear equivalent of the solutions derived by Ackerberg [1] for small values of the surface tension. The free-surface profiles have, in general, large capillary waves. Therefore they can only be used if the direction of the flow in Figure 1 is reversed.

2. Formulation

We consider the free-surface flow sketched in Figure 1. The flow is bounded below by the bottom EF and above by the walls AB and BC and the free surface CD. We neglect the effects of gravity, viscosity and compressibility, but we take into account the effect of surface tension. We introduce Cartesian coordinates with the origin at the separation point C. As $x \to -\infty$, the flow reduces to a uniform flow with velocity U and depth H.

We define dimensionless variables by choosing H as the unit length and U as the unit velocity. We introduce the potential function ϕ, the streamfunction ψ and the complex potential $f = \phi + \mathrm{i}\psi$. Without loss of generality we choose $\phi = 0$ at C and $\psi = 0$ on $ABCD$, which implies by the choice of dimensionless variables that $\psi = -1$ on the bottom, EF.

Next we introduce the complex velocity $u - iv$ where u and v are the horizontal and vertical components of the velocity respectively. We define a new complex function $\tau - \mathrm{i}\theta$ by the relation

$$u - \mathrm{i}v = \mathrm{e}^{\tau - \mathrm{i}\theta}. \tag{2.1}$$

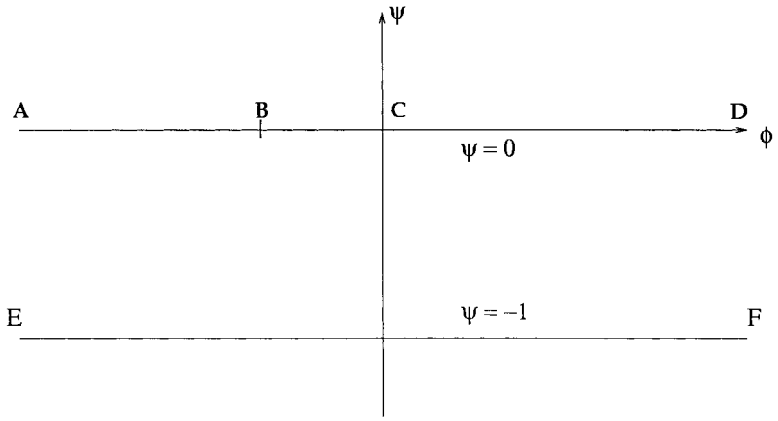

Figure 2. The complex potential f - plane.

Our aim is to calculate $\tau - i\theta$ as a function of $f = \phi + i\psi$ in the horizontal strip $-1 < \psi < 0$. On the free surface CD, the Bernoulli equation gives

$$\tfrac{1}{2}(u^2 + v^2) - \frac{TK}{\rho} = B^*. \tag{2.2}$$

Here T is the surface tension, K is the curvature, ρ is the density and B^* is the dimensional Bernoulli constant. Using the dimensionless variables we rewrite (2.2) as

$$\tfrac{1}{2}(u^2 + v^2) - \delta K = B^{**}, \tag{2.3}$$

where $\delta = T/HU^2\rho$ and $B^{**} = B^*/U^2$ is the dimensionless Bernoulli constant. Now, using (2.1) we get

$$u^2 + v^2 = e^{2\tau},\ K = -e^{\tau}\frac{\partial\theta}{\partial\phi}. \tag{2.4}$$

Therefore, (2.2) gives

$$\tfrac{1}{2}e^{2\tau} + \delta e^{\tau}\frac{\partial\theta}{\partial\phi} = B^{**}, \tag{2.5}$$

The kinematic conditions on the container ABC and the bottom EF imply that

$$v = 0 \qquad \text{on} \quad \psi = -1, \tag{2.6}$$

$$v = 0 \qquad \text{on} \quad \psi = 0,\ \phi < \phi_B, \tag{2.7}$$

and

$$u = 0 \qquad \text{on} \quad \psi = 0,\ \phi_B < \phi < 0. \tag{2.8}$$

We map the horizontal strip in Figure 2 onto the upper half of the complex plane $\zeta = \alpha + i\beta$ by the transformation

$$\zeta = \alpha + i\beta = e^{-\pi f} = e^{-\pi(\phi + i\psi)} = e^{-\pi\phi}(\cos(\pi\psi) - i\sin(\pi\psi)). \tag{2.9}$$

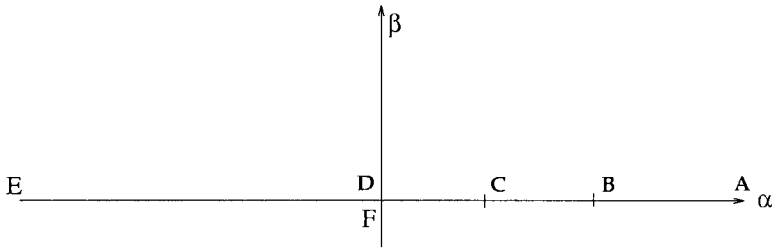

Figure 3. Flow configuration in the $\zeta = \alpha + i\beta$ plane.

The complex ζ-plane is sketched in Figure 3.

We apply the Cauchy integral formula to the function $\tau - i\theta$ in the complex ζ-plane with a contour consisting of the real axis and a semi-circle, centred at the origin and of arbitrary large radius extending into the upper half plane. Using the fact that $\tau - i\theta \to 0$ as $|\beta| \to \infty$, it can be shown that there is no contribution from the semi-circle. Therefore we have

$$\tau(\alpha) - i\theta(\alpha) = \frac{1}{\pi i}\int_{-\infty}^{\infty} \frac{\tau(\bar{\alpha}) - i\theta(\bar{\alpha})}{\bar{\alpha} - \alpha} d\bar{\alpha}, \tag{2.10}$$

where $\tau(\alpha)$ and $\theta(\alpha)$ denote the values of τ and θ on the axis $\beta = 0$. The integral in (2.10) is a Cauchy principal value. Taking the real part of (2.10) we obtain

$$\tau(\alpha) = -\frac{1}{\pi}\int_{-\infty}^{\infty} \frac{\theta(\bar{\alpha})}{\bar{\alpha} - \alpha} d\bar{\alpha}. \tag{2.11}$$

The kinematic boundary conditions (2.6) – (2.8) imply that

$$\theta(\alpha) = 0 \qquad \text{for} \quad \alpha < 0 \quad \text{and} \quad \alpha > \alpha_B \tag{2.12}$$

and

$$\theta(\alpha) = -\frac{\pi}{2} \qquad \text{for} \quad 1 < \alpha < \alpha_B. \tag{2.13}$$

Substituting (2.12) and (2.13) in (2.11) we obtain, after some algebra,

$$\tau(\alpha) = \frac{1}{2}\log\left|\frac{\alpha_B - \alpha}{1 - \alpha}\right| - \frac{1}{\pi}\int_0^1 \frac{\theta(\bar{\alpha})}{\bar{\alpha} - \alpha} d\bar{\alpha}. \tag{2.14}$$

Finally we revert to the variable ϕ by using the change of variable

$$\alpha = e^{-\pi\phi}. \tag{2.15}$$

This yields

$$\tau'(\phi_0) = \frac{1}{2}\log\left|\frac{e^{-\pi\phi_B} - e^{-\pi\phi_0}}{1 - e^{-\pi\phi_0}}\right| - \int_0^{\infty} \frac{\theta'(\phi)e^{-\pi\phi}}{e^{-\pi\phi} - e^{-\pi\phi_0}} d\phi\,, \tag{2.16}$$

where $\tau'(\phi) = \tau(e^{-\pi\phi})$ and $\theta'(\phi) = \theta(e^{-\pi\phi})$. We rewrite (2.5) in terms of τ' and θ' as

$$\frac{1}{2}e^{2\tau'} + \delta e^{\tau'}\frac{\partial\theta'}{\partial\phi} = B^{**}. \tag{2.17}$$

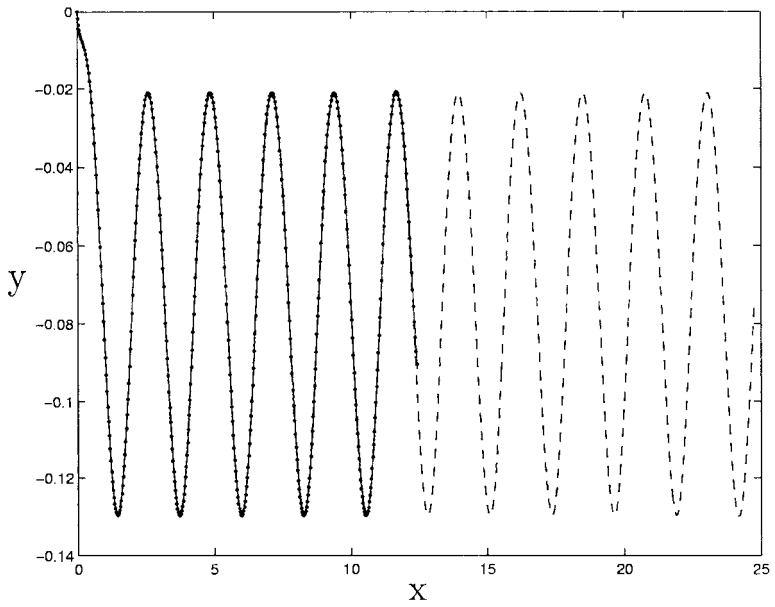

Figure 4. Analysis of accuracy of numerical method on a free surface profile

Substituting (2.16) in (2.17) define a nonlinear integral equation for the unknown function θ'. We shall refer to this equation as the equation Σ.

3. Numerical procedure

We solve the nonlinear integral equation Σ numerically. We first introduce equally spaced mesh points

$$\phi_I = (I-1)\Delta \qquad I = 1, \ldots, N \tag{3.1}$$

in the potential function ϕ. Here $\Delta > 0$ is the distance between mesh points. We also define the unknowns

$$\theta_I = \theta'(\phi_I). \tag{3.2}$$

Next we evaluate the values $\tau_{I+\frac{1}{2}}$ of $\tau'(\phi_0)$ at the midpoints

$$\phi_{I+\frac{1}{2}} = \frac{\phi_{I+1} + \phi_I}{2} \qquad I = 1, \ldots, N-1 \tag{3.3}$$

by using (2.16). This gives

$$\tau_I^m = \tau(\phi_{I+\frac{1}{2}}) = \frac{1}{2}\log\left|\frac{e^{-\pi\phi_B} - e^{-\pi\phi_{I+\frac{1}{2}}}}{1 - e^{-\pi\phi_{I+\frac{1}{2}}}}\right| - \int_0^\infty \frac{\theta'(\phi)e^{-\pi\phi}}{e^{-\pi\phi} - e^{-\pi\phi_{I+\frac{1}{2}}}}d\phi. \tag{3.4}$$

We approximate the integral in (3.4) by the trapezoidal rule with a summation over ϕ_I. Therefore we have

$$\tau_I^m = \frac{1}{2}\log\left|\frac{e^{-\pi\phi_B} - e^{-\pi\phi_{I+\frac{1}{2}}}}{1 - e^{-\pi\phi_{I+\frac{1}{2}}}}\right| - \sum_{j=1}^{N} \frac{\theta_j e^{-\pi\phi_j}\Delta w}{e^{-\pi\phi_j} - e^{-\pi\phi_{I+\frac{1}{2}}}} \qquad I = 1, \ldots, N-1, \tag{3.5}$$

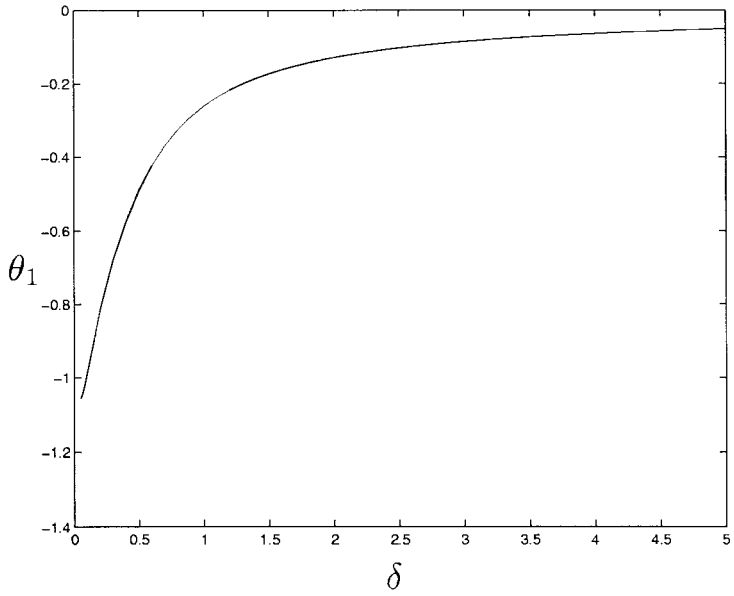

Figure 5. The change in θ_1 as the surface tension parameter δ is altered and $\alpha_B = 2{\cdot}0$.

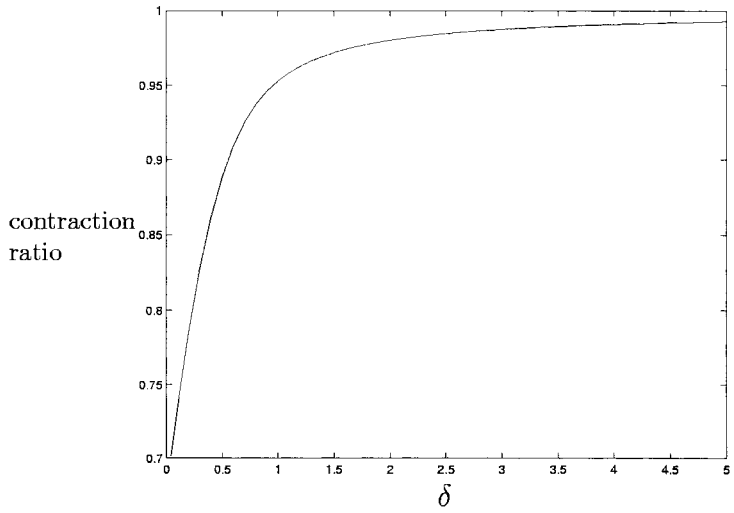

Figure 6. The change in the contraction ratio as the surface tension parameter δ is altered and $\alpha_B = 2{\cdot}0$.

where $w = 1/2$ for $j = 1, N$ and $w = 1$ otherwise.

Substituting (3.5) in (2.5) we obtain $N - 1$ nonlinear equations in the $N + 2$ unknowns θ_I for $I = 1, \ldots, N$, B^{**} and α_B. The last three equations are obtained by fixing θ_k for a fixed k, α_B, and the length l of the container edge BC. To calculate the length of the container edge BC, we define a uniform mesh on the interval $[1, \alpha_B]$, the image of BC in the ζ plane, by

$$\alpha_I = 1 + \frac{(\alpha_B - 1)}{(N_l - 1)}(I - 1), \qquad I = 1, \ldots, N_l. \tag{3.6}$$

Using (2.14) we calculate the value of τ at these points and then integrate the equation

$$\frac{\partial y}{\partial \alpha} = \frac{e^{-\tau}}{\pi \alpha}, \tag{3.7}$$

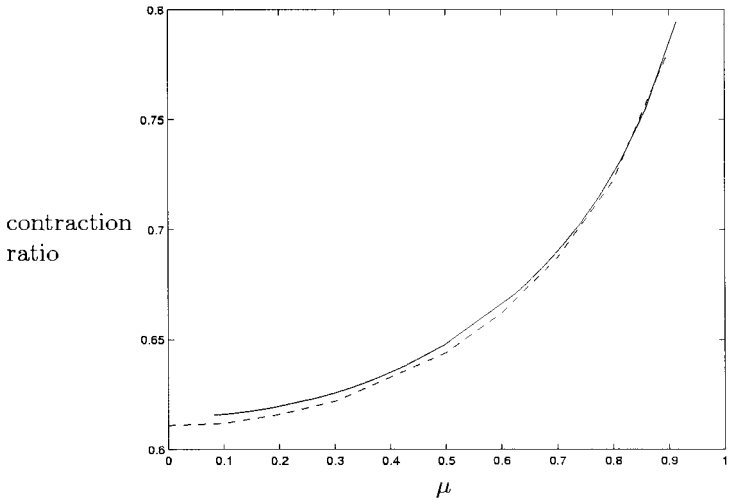

Figure 7. A Gurevich comparison for a waveless flow with zero surface tension, (Gurevich data is the broken line). Here μ is the ratio of the vertical distance from C to the wall EF and the upstream depth.

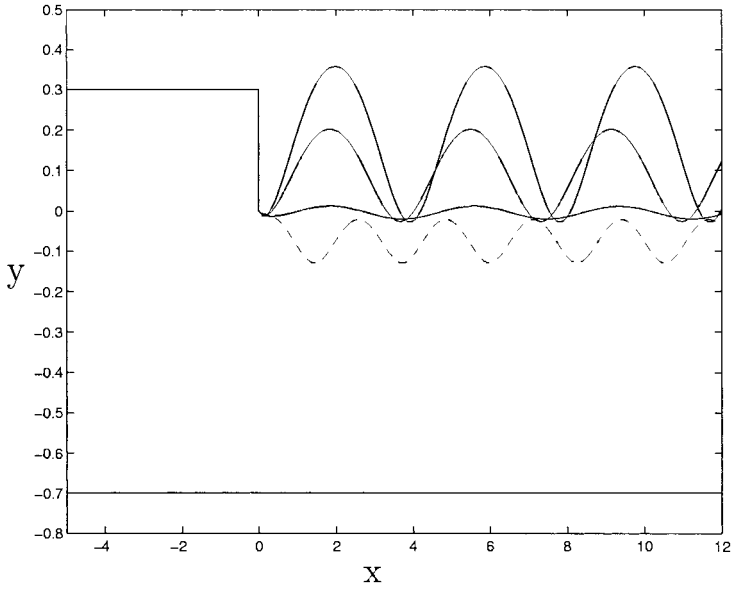

Figure 8. Flow profiles for $l = 0{\cdot}3$, $\alpha_B = 2{\cdot}0$, $\theta_{50} = 0{\cdot}01$ and varying δ. The solid lines going from top to bottom correspond to $\delta = 1{\cdot}0, 1{\cdot}1, 1{\cdot}5$. The corresponding values of the separation angle are $\theta_1 = -0{\cdot}29, -0{\cdot}25, -0{\cdot}18$. These are found as part of the solution. The broken line corresponds to $l = 0{\cdot}3$, $\alpha_B = 2{\cdot}0$, $\theta_{50} = 0{\cdot}01$, $\delta = 1{\cdot}0$ and $\theta_1 = 0{\cdot}20$, found as part of the solution.

on $[1, \alpha_B]$, with $y_C = 0$, to obtain y_B. Hence, the last equation is $l = y_B - y_C = y_B$, where l is fixed.

We now have a system of $N + 2$ nonlinear equations with $N + 2$ unknowns. This system is solved by Newton's method. Once a solution has been obtained, we can calculate the x and y coordinates by integrating the identities

$$\frac{\partial x}{\partial \phi} = e^{-\tau} \cos\theta, \tag{3.8}$$

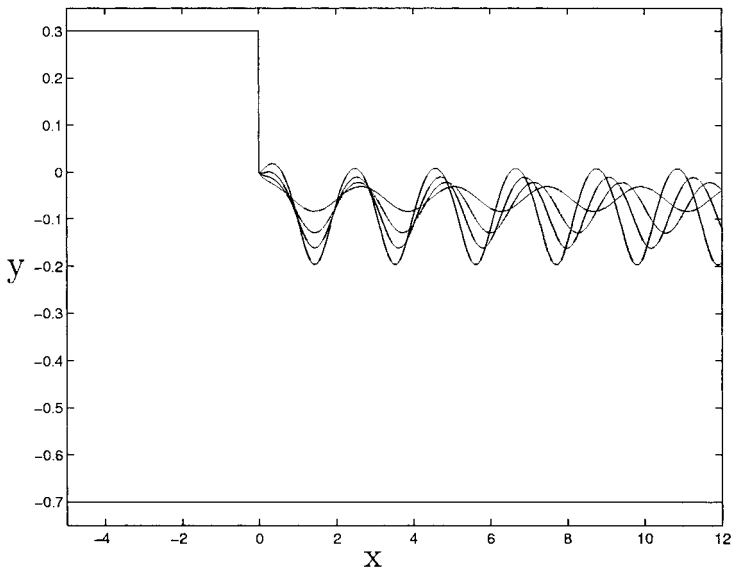

Figure 9. Flow profiles for $\delta = 1{\cdot}0$, $l = 0{\cdot}3$, $\theta_{50} = 0{\cdot}01$ and varying α_B. From top to bottom (increasing amplitude) $\alpha_B = 1{\cdot}98, 2{\cdot}0, 2{\cdot}02, 2{\cdot}05$. The corresponding values of the separation angle are $\theta_1 = -0{\cdot}24, -0{\cdot}20, -0{\cdot}16, -0{\cdot}10$. These are found as part of the solution

$$\frac{\partial y}{\partial \phi} = \mathrm{e}^{-\tau} \sin\theta. \tag{3.9}$$

This gives the recursive relation s

$$x_{I+1} = x_I + \Delta \mathrm{e}^{-\tau_{I+\frac{1}{2}}} \cos\theta_{I+\frac{1}{2}}, \tag{3.10}$$

$$y_{I+1} = y_I + \Delta \mathrm{e}^{-\tau_{I+\frac{1}{2}}} \sin\theta_{I+\frac{1}{2}}. \tag{3.11}$$

4. Results

An important question is the number of parameters we need to specify to determine unique solutions. Our numerical results show that there is a two-parameter family of waveless solutions and a four-parameter family of solutions with a train of capillary waves as $x \to \infty$. Furthermore the waveless solutions are particular limiting cases of the four-parameter family of solutions as the amplitude of the waves approaches zero. We found that the numerical schemes do not converge as $N \to \infty$ when more or less parameters are fixed.

For the four-parameter problem, the solutions where we allow waves to form on the free surface, we analysed the accuracy of the numerical method used. In Figure 4, we show the effect of truncation and mesh size on an example of a free surface profile corresponding to $\delta = 1{\cdot}0$, $\alpha_B = 2{\cdot}0$, $l = 0{\cdot}30$ and $\theta_k = 0{\cdot}01$ where k is defined such that θ_k is the value of θ at $\phi = 2{\cdot}45$. For example, this means that $k = 50$ for $\Delta = 0{\cdot}05$ and $k = 99$ for $\Delta = 0{\cdot}025$. The dots mark out a profile that is made up of $N = 400$ mesh points, with a mesh size of $\Delta = 0{\cdot}05$. The dashed line is for the same mesh size, but double the number of points, *i.e.* $N = 800$. The final profile which is the solid line is for $N = 800$ mesh points and a mesh

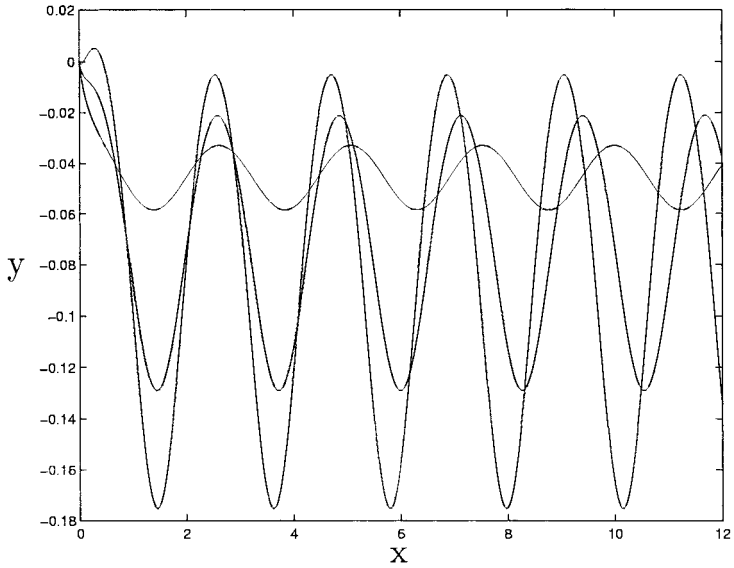

Figure 10. Flow profiles for $\delta = 1{\cdot}0$, $\theta_{50} = 0{\cdot}01$, $\alpha_B = 2{\cdot}0$ and varying l. From top to bottom (increasing amplitude) $l = 0{\cdot}305, 0{\cdot}30, 0{\cdot}295$. The corresponding values of the separation angle are $\theta_1 = -0{\cdot}27, -0{\cdot}20, -0{\cdot}14$. These values are found as part of the solution.

size $\Delta = 0{\cdot}025$. The three sets of results agree within graphical accuracy. This illustrates the convergence of the scheme as $N \to \infty$ and $\Delta \to 0$. Most of the results presented here were obtained with $N = 500$ and $\Delta = 0{\cdot}05$.

To calculate the two-parameter family of waveless solutions, we impose the condition that there are no waves as $x \to \infty$ by requiring $\theta_{N-1} = \theta_N$. We found that, in the absence of waves, the free surface does not leave the wall tangentially unless $T = 0$. In other words $\theta_1 \neq -\pi/2$ when $T \neq 0$. This is illustrated in Figure 5 where we present values of θ_1 against values of δ. As $\delta \to 0$, $\theta_1 \to -\pi/2$ and as $\delta \to \infty$, $\theta_1 \to 0$. The limiting case $\delta = \infty$ corresponds to a horizontal free surface. When $\alpha_B \to \infty$ and $\delta \to 0$, the waveless results reduce to those of Vanden-Broeck [3]. We also calculated the contraction ratio defined as the thickness of the stream as $x \to \infty$ divided by the vertical distance from C to the wall EF (see Figure 1). The contraction ratios can be compared with the data obtained by Gurevich [13, pp. 71–78], using free-streamline theory. In Figure 7 we plot contraction ratio against μ, where μ is the ratio of the vertical distance from C to the wall EF and the upstream depth. Here we can see that for $T = 0$, we recover the classical value for the contraction ratio of $\pi/(\pi + 2)$ as $\mu \to 0$.

The four-parameter family of solutions are presented in Figures 8–10. These results were obtained with $N = 500$ and $\Delta = 0{\cdot}05$. The four parameters are chosen as δ, α_B, l and θ_{50}. There is no special physical meaning associated with θ_{50} and a value θ_k with $k \neq 50$ or another quantity could have been chosen as the fourth parameter. In each of the Figures 8–10, we fix three parameters and show the effect of varying the fourth. In all of the results presented, $\theta_1 \neq -\pi/2$, so that the free surface does not leave the wall tangentially. As mentioned at the end of the introduction, solutions with $\theta_1 = -\pi/2$ are of particular interest since there is no singularity at C. However, the results in Figure 8 show that the amplitude of the wave increases rapidly as θ_1 approaches $-\pi/2$. The dashed line and one of the solid lines in Figure 8 corresponds to the same values of the parameters, namely $\alpha_B = 2{\cdot}0$, $l = 0{\cdot}3$, $\delta = 1{\cdot}0$ and

$\theta_{50} = 0{\cdot}01$. These parameter values give a non unique solution. What we use as an initial guess in our numerical scheme, determines which free-surface profile is produced. Due to these capillary waves on the free-surface, it must be remembered that these profiles are only valid if the flow direction of Figure 1 is reversed.

5. Conclusion

We have explored the problem of flow from a container, using this as an example of a more general problem involving rigid wall and free-surface interaction. We have shown that there is a four-parameter family of solutions. These solutions are, in general, singular at the separation point and have capillary waves on the free-surface. They include as a particular case of waveless solutions of Vanden-Broeck [3].

Acknowledgements

The work was supported by EPSRC.

References

1. R. C. Ackerberg, The effects of capillarity on free-streamline separation. *J. Fluid Mech.* (1975) 333–352.
2. E. Cumberbatch and J. Norbury, Capillary modification of the singularity at a free-streamline separation point. *Q. J. Mech. Appl. Math.* 32 (1979) 303–312.
3. J.-M. Vanden-Broeck, The effect of surface tension on the shape of a Kirchhoff jet. *Phys. Fluids.* 27 (1984) 1933–1936.
4. R. C. Ackerberg, The effects of capillarity on the contraction coefficient of a jet emanating from a slot. *Phys. Fluids* 30 (1986) 289–296.
5. J.-M. Vanden-Broeck, The influence of capillarity on cavitating flow past a flat plate. *Q. J. Mech. Appl. Math.* 34 (1981) 465–473.
6. C. D. Andersson and J.-M. Vanden-Broeck, Bow flows with surface tension. *Proc. R. Soc. London* A452 (1996) 1985–1997.
7. G. D. Crapper, An exact solution for progressive capillary wave of arbitrary amplitude. *J. Fluid Mech.* 2 (1957) 532–540.
8. L. K. Forbes and L. W. Schwartz, Free-surface flow over a semicircular obstruction. *J. Fluid Mech.* 114. (1982) 299–314.
9. D. I. Meiron, G. R. Baker and S. A. Orszag, Generalized vortex methods for free-surface flow problems. *J. Fluid Mech.* 123 (1982) 477–501.
10. D. I. Meiron and P. G. Saffman, Overhanging interfacial gravity waves of large amplitude. *J. Fluid Mech.* 129 (1983) 213–218.
11. A. C. King and M. I. G. Bloor, Free-surface flow over a step. *J. Fluid Mech.* 182 (1987) 193–208.
12. J.-M. Vanden-Broeck, Cavitating flow of a fluid with surface tension past a circular cylinder. *Phys. Fluids* 3 (1990) 263–266.
13. M. I. Gurevich, *Theory of Jets in Ideal Fluids.* New York, London: Academic Press (1965) 585 pp.